

Measurement and simulation of temperature and velocity fields during the cooling of water in a die casting model

S. Eck*, M. Stefan Kharicha, A. Ishmurzin, A. Ludwig

University of Leoben, Department of Metallurgy, Franz-Josef Str. 18, 8700 Leoben, Austria

Abstract

Simultaneous measurements of temperature and velocity fields have been performed by applying combined laser induced fluorescence (LIF) and particle image velocimetry (PIV) techniques to natural convection in a die cast model. A 10 cm × 10 cm × 3 cm U-shape rectangular die casting model has been filled with pure water and the cell walls have been continuously cooled between 41 and 6 °C. The resulting natural convection pattern and temperature field have been measured with PIV and LIF. Furthermore, the convection pattern has been simulated in 2D and 3D using the commercial CFD software FLUENT. The comparison of the experimental and numerical results given in this work shows good agreement both qualitatively and quantitatively.

© 2005 Elsevier B.V. All rights reserved.

Keywords: Convection; Water; Die casting model; Particle image velocimetry (PIV); Laser induced fluorescence (LIF); CFD calculation

1. Introduction

The two phase model proposed by Ludwig et al. [1–4] has been successfully applied to globular equiaxed solidification. The model considers nucleation and growth of equiaxed grains, motion and sedimentation of grains, feeding flow and solute transport by diffusion and convection. It allows the prediction of macrosegregations and the distribution of grain size. Whether the Eulerian multiphase model can be successfully applied to the solidification and phase separation processes is strongly dependent on the definition and implementation (through user defined subroutines) of source terms, interaction terms, and other auxiliary terms into the conservation equations. Thus, experiments with the same boundary conditions are essential to verify the numerical predictions. In a recent publication, we presented an experimental observation study of convection during equiaxed solidification of transparent alloys [5]. There, 3D samples of NH₄Cl–H₂O solutions were solidified under defined experimental conditions. The occurring melt convection had been investigated by particle image velocimetry (PIV). Fig. 1 shows PIV results measured during the early stage of the solidification process when the formation of crystals was observed at the cell walls, forming a columnar zone. The convectional field in the measurement cell at this stage showed two major vortices

with downward streaming at the cold walls and upward streaming in the centre of the measurement cell. The occurrence of NH₄Cl crystals was observed optically and first attempts were made to quantitatively measure their number density, size distribution and sedimentation rate by PIV and particle tracking (PT). The aforementioned study demonstrated the applicability of particle image velocimetry and particle tracking in a solidification experiment. It illustrated that the convectional flow field, particle numbers and sizes can be quantified with these techniques. The aim of the experiments which we present in the present paper is to further investigate the temperature and velocity fields of the stable convection rolls that had been observed prior to solidification. A quantification of the temperature and the occurring velocities in the convection rolls should be compared with CFD calculations of the same system. The combination of experimental and numerical results will lead to a better understanding of the process as well as improvements to our numerical model. Since the influence of Rhodamine on the NH₄Cl–water solidification has not yet been explored, we started with PIV and LIF investigations of pure water, where the same convection rolls have been observed as in the early stage of NH₄Cl–H₂O solidification.

2. Experimental techniques and setup

Particle image velocimetry (PIV) is a whole-flow-field technique providing instantaneous velocity vector measurements in a cross-section of a flow. The use of modern CCD cameras

* Corresponding author. Tel.: +43 38424 022 223.
E-mail address: sven.eck@unileoben.ac.at (S. Eck).

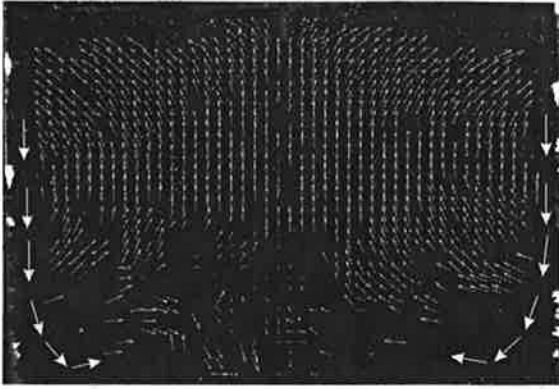


Fig. 1. PIV results measured during the early $\text{NH}_4\text{Cl-H}_2\text{O}$ solidification process, see Ref. [5].

and dedicated computing hardware results in real-time velocity maps. The measurement principle of PIV has been presented in a former publication [5]. Planar laser induced fluorescence (P-LIF) is an image acquisition method which enables visualization and quantitative measurements of concentration or temperature fields. In our experiments, we took advantage of the temperature dependence of the fluorescence intensity of Rhodamine B. The experimental procedure will be described in the following section. For the PIV and LIF experiments presented in this study we used a double cavity Nd-YAG Laser (frequency doubled, $\lambda = 532 \text{ nm}$). The data analysis for PIV was performed using the commercial software package “FlowManager”, provided by DANTEC dynamics [6]; the data analysis for P-LIF was performed via a self-developed image processing script written in MATLAB. A square measurement cell with $10 \text{ cm} \times 10 \text{ cm} \times 3 \text{ cm}$ inner diameter was designed with three copper walls and two transparent sides made of glass. Front and top view of the measurement cell are shown in Fig. 2 together with a sketch of the setup for stereoscopic PIV/LIF. The three copper walls of this measurement cell can be cooled and heated separately or together in a controlled manner. The coolant used consisted of a mixture of water and automotive anti-freeze. It could be heated/refrigerated between $+150$ and $-35 \text{ }^\circ\text{C}$ and pumped by an external bath (HAAKE C30P) through silicone tubes into the cell walls. Inside the copper walls the coolant followed a meander path which led to a uniform temperature at the inside of the cell walls. The temperature of the cell walls and for

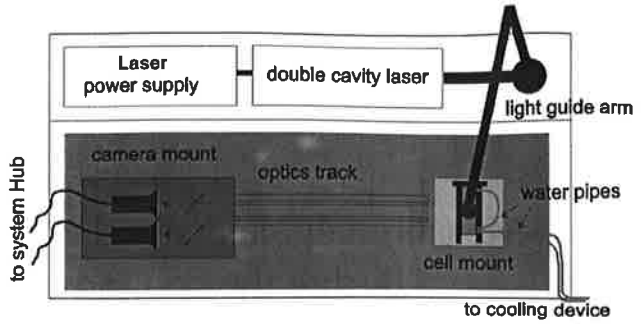


Fig. 3. Sketch of the combined PIV-LIF setup.

some checking experiments inside the measurement cell were measured and recorded via a 16 channel thermocouple reader (Stanford SR 630) equipped with NiCr-Ni (type K) thermocouples. For the experiments presented in this work, two identical cameras were mounted on a 50% beam splitter with the optical axis perpendicular to the glass plates of the measurement cell (Fig. 3). The camera lens of the PIV camera was covered by a band pass filter around $\lambda = 532/533 \text{ nm}$, the camera lens of the LIF camera was covered by a high pass filter $\lambda = 570 \text{ nm}$. In this way, the PIV camera only recorded direct or scattered light from the laser source, whereas the LIF camera only recorded the fluorescence of Rhodamine B.

2.1. Temperature field measurement (LIF)

Temperature levels are deduced from the local fluorescence re-emitted by the temperature sensitive marker Rhodamine B which is excited by a laser ($\lambda = 532 \text{ nm}$, $P_0 = 1\text{--}100 \text{ mW}$). The local fluorescence level depends on the Rhodamine concentration as well as on the exciting laser power. For a set of experiments, we therefore kept the laser power and the experiment geometry (camera setup and focus position) fixed. Preliminary experiments showed that the temperature field in the measurement cell within 1 min can be considered as constant. The LIF images shown in this work represent the calculated mean pixel value images of 50 sequential images, i.e. averaged over 50 s. This procedure was applied for both the LIF calibration and evaluation. For a medium laser power ($P_0 = 20\text{--}50 \text{ mW}$), the fluorescence increased linearly for small concentrations but reached a saturation at higher concentrations. For our combined PIV-LIF

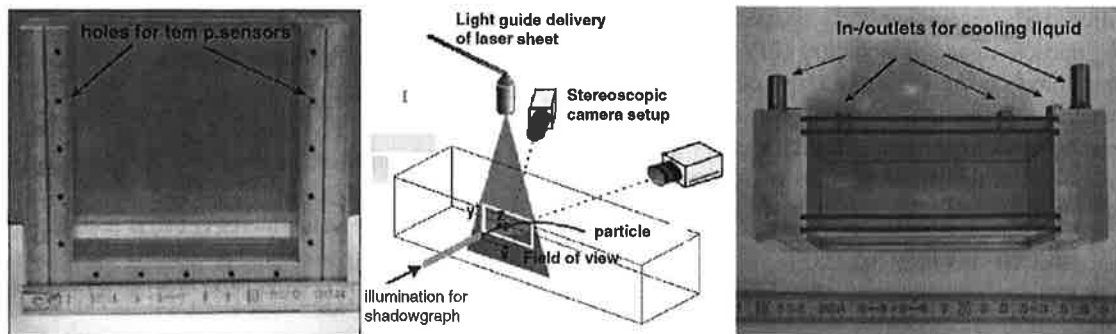


Fig. 2. Front and top views of the measurement cell and sketch of a stereoscopic PIV setup.

measurement, we chose a concentration of 90 $\mu\text{g/l}$ to avoid the saturation regime.

2.2. Velocity measurements (PIV)

In the present study, polyamide particles of 20 μm diameter were used for the velocity measurements. The average flow velocity during the convection experiments in our setup was in the order of 10^{-3} m/s. These seeding particles were chosen because the flow velocity was considerably higher than the particle settling velocity (for water in the order of 10^{-6} m/s as given in [7]). For PIV, the time between pulses was set to 1 s. The processing technique used in this study was Dantec's "adaptive correlation", a cross-correlation method described in [6]. The interrogation area was 32×32 pixels, i.e. 1.5 mm \times 1.5 mm, using three refinement steps, starting at 256×256 pixels. The overlaps of the interrogation area in the horizontal and vertical directions were 25 and 50%, respectively. Furthermore, a filter was applied, which filters out vector maps by arithmetic averaging over vector neighbors; an averaging area of 3×3 was used. This filter removed outliers due to false correlations resulting from reflections at the cell walls.

2.3. Measurement procedure

In agreement with the $\text{NH}_4\text{Cl-H}_2\text{O}$ solidification experiments the temperature range of interest was 5–45 $^\circ\text{C}$. For our PIV/LIF investigations we filled the measurement cell with 200 ml of distilled water and added 90 $\mu\text{g/l}$ Rhodamine B. The LIF calibration was done by a self-developed MATLAB script. In brief, the fluorescence intensity was plotted versus the corresponding temperature for three different temperatures: 5, 15, and 45 $^\circ\text{C}$. The script correlated the fluorescence intensity to the temperature at each pixel of the image via a linear fit. This correlation was stored and applied to LIF images taken with the same setup, i.e. the same Rhodamine concentration, camera setup and laser intensity. For the convection experiments, the water was left for several minutes at 41 $^\circ\text{C}$ until the movements from the

stirring had settled. When the PIV showed a random but low velocity distribution, the cooling of the cell walls was started. When setting the cooling water reservoir from 42 to 5 $^\circ\text{C}$ at maximum flow rate and cooling power, the coolant cooled the copper cell walls almost linearly from 40.7 to 6 $^\circ\text{C}$ within 1500 s and stayed at 6 $^\circ\text{C}$ for the rest of the experiment. The slope of the cell wall temperature was fit by a line with the simple equation $T(t) (^\circ\text{C}) = 40.29 (^\circ\text{C}) - 0.020 (\text{K/s}) \times t (\text{s})$. The result of the temperature measurement at the cell walls and a linear fit for the first 1500 s are shown in Fig. 4. Due to the good thermal conductivity of copper the walls the temperature differences along the cell walls were ≤ 0.2 K, as revealed by thermocouple measurements. As soon as the cooling of the wall had been started, PIV and LIF images were recorded.

3. Numerical simulation setup

The numerical simulation of natural convection of water in the die casting model was performed using the commercial CFD software FLUENT [8]. The density of water was taken as piecewise-linear temperature dependent [9]. The flow was calculated both in 2D and 3D and assumed to be laminar. The results of 2D and 3D calculations were found to be equivalent. Since the temperature field of the cavity was axis symmetric, the numerical simulation was chosen to compute only half the experimental cell, i.e. a 50 mm \times 65 mm rectangle represented the 2D computational domain. The computational grid was structured quadrilaterally, accordingly refined near the top, left, and the bottom walls, in order to resolve sharp temperature gradients at these borders. On the side and bottom planes of the cell, the temperature for each time step was assumed to be constant. At the upper surface of the cell, convective heat transfer between air and water was assumed, with a heat transfer coefficient of 100 $\text{W}/(\text{m}^2 \text{K})$, the temperature of the free air was taken as 20 $^\circ\text{C}$ (RT), and the free slip condition was taken for the velocity at this interface. As the initial condition, the temperature of water within the computational domain was set to 40.3 $^\circ\text{C}$, whereas velocities were set to zero. The time dependent boundary condition for the wall temperature given in Fig. 4 has been implemented in the FLUENT calculation via a user defined subroutine (UDF) [8].

4. Experimental results

In Fig. 5, we present the results of PIV velocity field and LIF temperature field measurements from 600 and 1500 s after the cooling of the cell walls began. The measured velocity vectors in Fig. 5(a, b, and e) are displayed in a rainbow color scheme where red corresponds to the highest and blue to the lowest velocity. A more quantitative description of the velocity field will be given in the comparison with the numerical results. The measured LIF temperature fields given in Fig. 5(c and d) are displayed with their corresponding color bar, where red corresponds to high and blue to low temperatures. The initial state PIV, i.e. 1–100 s after the start of the cooling showed a random distribution of velocity vectors in the order of 0.1 mm/s and a uniform temperature field of 40.7 $^\circ\text{C}$ (not shown). A visual

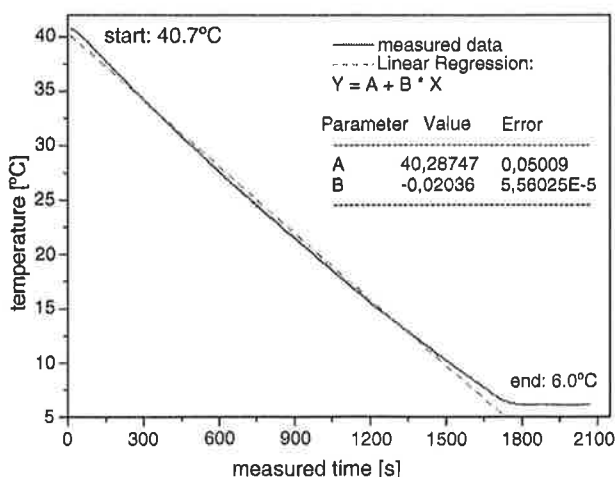


Fig. 4. Measured and approximated cell wall temperature.

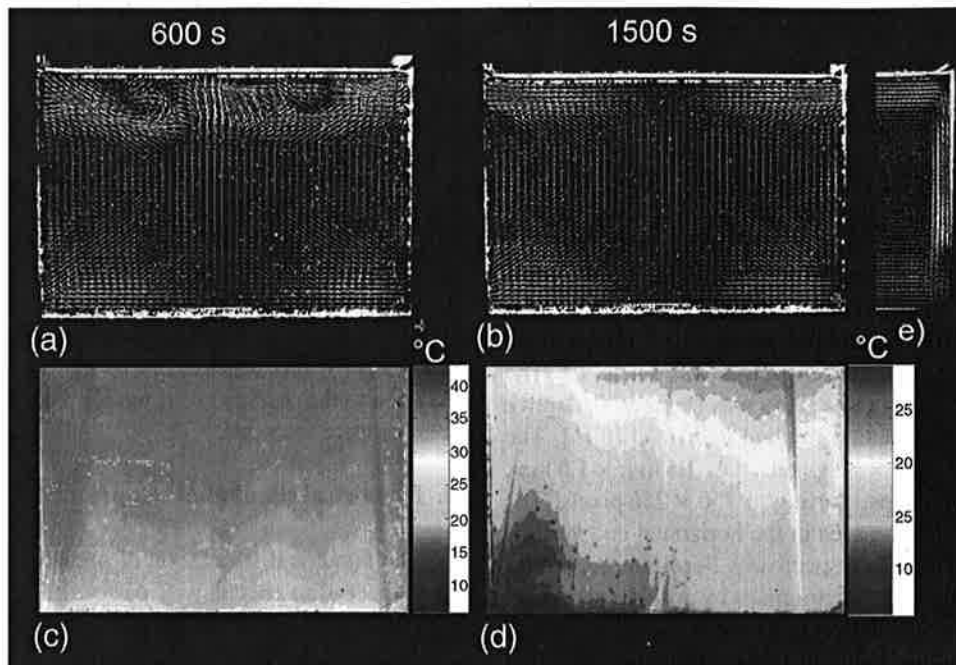


Fig. 5. PIV (a, b, e) and LIF (c and d) results of natural convection of water, details in the text.

observation of the particle flow showed the development of two convection rolls after 300–600 s. The established temperature gradient led to small changes of density which, in turn, created buoyancy forces that drive the flow of the liquid. At this stage the two clearly distinguishable convection rolls appeared in the instantaneous PIV measurements together with an unstable velocity region near the liquid–air interface at the top of the measurement cell (Fig. 5a). The LIF temperature field of this stage is given in Fig. 5c). The temperature field gradually changed from 30 °C at the bottom to 40 °C at the top with horizontal isolines in the centre and decreasing temperature close to the cooled side walls of the cell. The vertical lines visible as fan with darker rays in Fig. 5(c and d) are artefacts due to shadowing from particles floating at the liquid–air interface. A 1500 s after the start of the cell cooling, the visual observation and PIV showed two stable and axis symmetric convection rolls forming a centre region of low velocity in the order of 0.1 mm/s, accompanied by higher velocity regions (0.5–1 mm/s) in the corners of the measurement cell (Fig. 5b). The LIF taken at this stage is given in Fig. 5(d); the temperatures in the water at this stage ranged from 15 to 30 °C, the observed unsymmetry between the right and the left side of the cell are considered as an artefact due to an uneven illumination, however a tendency to horizontal isolines is still visible. In the visual observation of the process the convection rolls clearly reveal a down-flow near the cell walls and an up-flow in the centre of the measurement cell. When dividing the images into 32×32 pixel regions, the interrogation areas for the actual PIV correlation led to correlation problems near the cell walls which rendered the down-flow occurring close to the wall invisible. After ~ 60 min, i.e. when a steady-state temperature was reached, the down-flow near the cell side wall was wide enough to be measured with PIV as shown in Fig. 5(e).

5. Comparison of experimental and simulation results

In Fig. 6, we present the results of the numerical simulation, where Fig. 6(a and b) show the velocity and Fig. 6(c and d) the temperature fields at 600 and 1500 s, respectively. Comparison of Figs. 5 and 6 shows a good qualitative agreement of the measured and calculated velocity fields and temperature intervals within the cell. The best agreement was achieved 1500 s after the start of the cooling when a stable state was obtained in the experiment. To judge the agreement more quantitatively, velocity profiles have been extracted from the experimental and numerical results. In Fig. 7, we present velocity profiles displaying the length of the measured velocities along five vertical lines at 1–5 cm distance from the right cell wall. The 5 cm line profile thus represents velocities measured on the vertical center line of our measurement cell, i.e. the symmetry line of the numerical setup. The experimental and numerical results are displayed in Fig. 7(a and b), respectively. On the centre line the measured velocities ranged from 0 to 0.1 mm/s with a maximum in the centre and minima on the top and the bottom. Going from the centre towards the wall the line profiles show a constant value around 0.1 mm/s as minimum in the centre and maxima up to 0.8 mm/s near the top and 0.4 mm/s in the bottom region. The fact that the two top corners showed velocities which were by a factor of ~ 2 higher than the bottom corners is attributed to the different interface conditions. At the top, the liquid air friction facilitates the flow as compared to the liquid-wall friction at the bottom and the side walls. In the numerical simulation this behavior was taken into account by assuming a non-slip condition at the cell walls and a slip condition at the top in the simulation setup. The fact that the experimental velocity curves show kinks at the top and bottom interface is attributed to PIV correlation problems

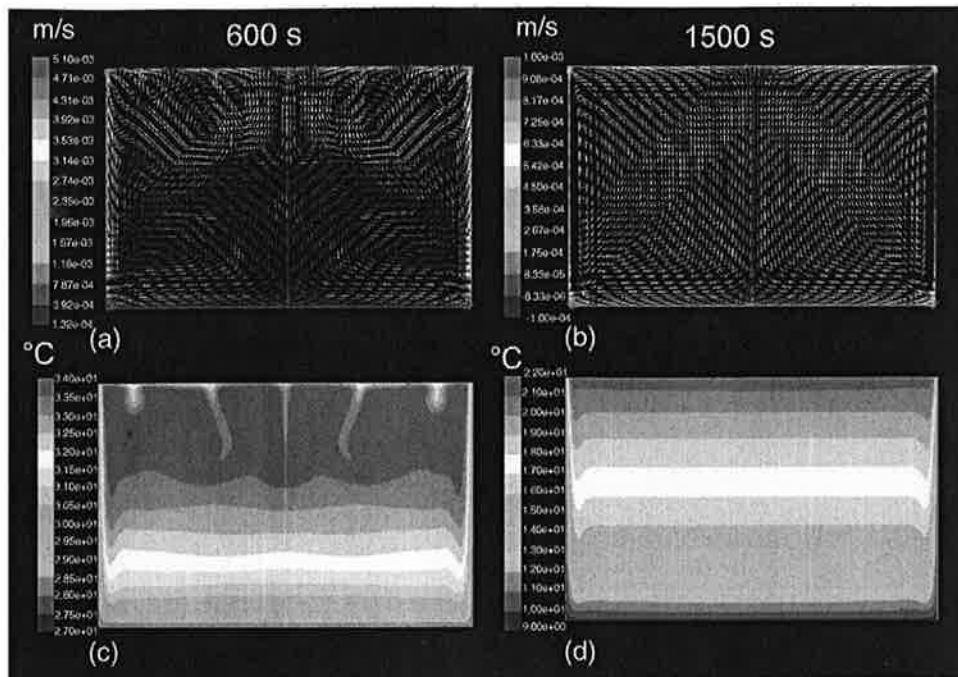


Fig. 6. CFD calculated velocity and temperature fields in water after 600 s (a and c) and 1500 s (b and d).

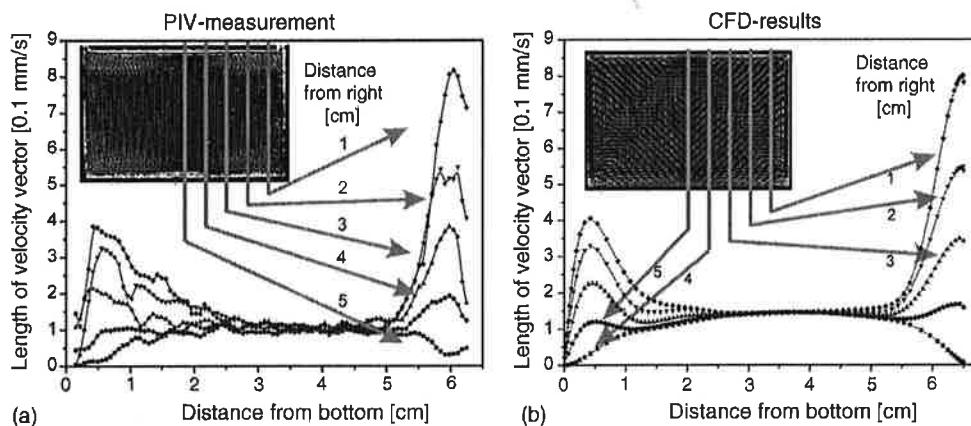


Fig. 7. Velocity distribution along vertical lines at the given distances from the right cell wall.

which arise due to reflections at the cell wall and the liquid–air interface.

6. Summary and outline

Simultaneous measurements of temperature and velocity fields have been performed applying a combined laser induced fluorescence (LIF) and particle image velocimetry (PIV) setup to natural convection in a die casting model. Furthermore, the natural convection has been modeled numerically using a single phase model. The work illustrated the difficulties to get reasonable experimental results on one hand and to choose proper boundary conditions and material properties for numerical simulations on the other hand. The achieved agreement between numerical prediction and experimental results confirms the applicability of the reported setups as starting points for both experimental and numerical investigations of the convection dur-

ing hypereutectic $\text{NH}_4\text{Cl-H}_2\text{O}$ solidification in our die casting model.

Acknowledgements

This work has been funded by the Austrian Science Funds (FWF) [10] and was supported by the Austrian Christian Doppler (CD) Research Association in the frame of the CD Laboratory “Multiphase Simulation of Metallurgical Processes”.

References

- [1] A. Ludwig, M. Wu, *Metall. Mater. Trans. A* 33 (2002) 3673–3683.
- [2] M. Wu, A. Ludwig, A. Bührig-Polaczek, *Solidification and Crystallization*, in: D. Herlach (Ed.), 2004, pp. 204–212.
- [3] M. Wu, A. Ludwig, *Adv. Eng. Mater.* 5 (2003) 62–66.
- [4] M. Wu, A. Ludwig, A. Bührig-Polaczek, P.R. Sahn, *Inter. J. Heat Mass Transfer* 46 (15) (2003) 2819–2832.

- [5] S. Eck, J. Mogeritsch, A. Ludwig, *Mater. Sci. Forum* 508 (2005) 157–162.
- [6] FlowManager software and Introduction to PIV Instrumentation, Dantec Dynamics GmbH, Publ. No.: 9040U3625, 2000.
- [7] C. Ghenai, A. Mudunuri, C.X. Lin, M.A. Ebadian, *Exp. Therm. Fluid Sci.* 28 (1) (2003) 23–35.
- [8] FLUENT 6.2 UDF Manual, Fluent Inc., 2005.
- [9] J.A. Dean, *Lange's Handbook of Chemistry*, McGraw-Hill Inc., 1999.
- [10] Fonds zur Förderung der wissenschaftlichen Forschung (FWF), Projekt 17619, <http://www.fwf.ac.at>.